Amperometric Electrochemical Sensor Array for On-Chip Simultaneous Imaging : Circuit and Microelectrode Design Considerations

Junichi Hasegawa, Shigeyasu Uno and Kazuo Nakazato

Nagoya Univ. Dept. of Electrical and Computer Science. Graduate School of Eng.
Furo-cho, Chikusa-ku, Nagoya, Aichi 464-8603, Japan
Phone: +81-52-789-2794 Fax: +81-52-789-3139
E-mail: j_hasega@echo.nuee.nagoya-u.ac.jp, nakazato@nuee.nagoya-u.ac.jp

1. Introduction

The development of array-based biosensors has received considerable attention due to the strong demand for rapid and high-throughput analyses [1] [2]. Fluorescence measurement has a high sensitivity. However, it has some drawbacks such as shielding by a turbid solution or vessels and need for labeling nonfluorescent species. An electroanalytical detection method offers advantages over optical methods, including the elimination of optical interference and low cost. Electrochemical devices with microelectrode arrays (MEAs) have substantial advantages such as local analysis and steady-state current. The principle of amperometry is based on the measurement of the current induced by a redox reaction at the working electrode (Fig. 1). A microelectrode has a steady-state current response in unstirred solutions and huge addressable microelectrodes can be incorporated into an integrated circuit [3]. However, as it takes a few or tens of seconds before reaching a steady-state current, rapid multipoint measurement is impossible by the simple switching scheme. In this work, we introduce amperometric electrochemical sensor circuit for rapid and simultaneous measurement. We also propose a novel microelectrode structure to suppress diffusion layer expansion over MEA, which is verified by computer simulation.

2. Amperometric Sensor Circuit

In our amperometric sensor circuit, each electrode is connected to two switches (Fig. 2). An electrode under measurement is connected to the readout circuit via "switch A", and during stand-by the potential is fixed to maintain steady-state current via "switch B". Hereby we need not wait for steady-state current, realizing ultra-fast readout from each electrode. In order to suppress electrode potential variation by switching, current buffer circuit is inserted between each electrode and switches. This current buffer circuit employs the source follower to fix electrode potential at V_{el}, as well as the current mirror to copy current ($I_{out}=I_{in}$) (Fig. 3(a)). Simulation result of the current buffer circuit shows that input current range is between 10 pA and 100 μA, and measurement agrees well with simulation in the range between 1 nA and 100 μA (Fig. 4(a)). Fig. 4(b) shows the time course of the electrochemical current of 100 mM Na_2SO_4 measured using the current buffer circuit. The output current increases with increasing electrode size, which indicates successful measurement of electrolyte solution using the current buffer circuit.

3. Simulation of Amperometry Using MEA

In case of the constant potential measurement, applying the potential to all electrodes in the array leads to continuous expansion of the diffusion layer around each microelectrode. The diffusion layers of the closely spaced microelectrodes overlap, and the current magnitudes start to decrease continuously, which makes local and quantitative analysis extremely difficult (Fig. 5(a)). Our working electrode is surrounded by a grid auxiliary electrode. Therefore redox cycling occurs between the electrodes, and diffusion layer is confined (Fig. 5(b)). In order to verify this, amperometry at MEA was simulated by COMSOL Multiphysics using the model described in Figs. 6(a) and (b). Figs. 7 (a) and (b) show color maps of simulated concentration profiles along a side of the unit cell. For conventional MEA, the diffusion layers of the closely spaced microelectrodes overlap and planar diffusion layer is formed. On the other hand, our MEA shows suppression of diffusion layer expansion due to grid auxiliary electrodes, and hemispherical diffusion layers are formed on individual microelectrode. On conventional MEA, steady-state current is not observed and the current magnitude continuously decreases (Fig. 8, green). On the other hand, our MEA shows a steady-state current (blue). Furthermore, the steady-state current is amplified compared to single microelectrode (red), and the time to reach the steady-state is reduced to about 1/10 of that of single microelectrode. Fig. 9 shows the current gain of our MEA, defined as the ratio of steady-state current to that of single microelectrode. Gain depends on the ratio of three characteristic lengths of geometry; $L_{WE}:L_{gap}:L_{AE}$, rather than the absolute lengths (Fig. 9). Fig. 10 shows that the gain saturates at $L_{WE}/L_{AE}=1.0$, and L_{gap}/L_{WE} decreases further, larger amplification is observed.

4. Conclusion

We have proposed amperometric electrochemical sensor circuit for rapid and simultaneous measurement, as well as and a novel microelectrode structure to suppress diffusion layer expansion over MEA. Each electrode has a steady-state current, which is amplified, and the time to reach the steady-state is reduced to about 1/10 of that of single microelectrode.

References

[1] C.B.Davis, et al., Biosens. Bioelectron. 18 (2003) 1299.
[2] J.K.Nga, et al., Biosens. Bioelectron. 23 (2008) 803.
[3] R.Kakerow, et al., Sensors and Actuators A. 43 (1994) 296

Solution
Red   Ox
Electrode
Insulator e^-
Current

2D mapping
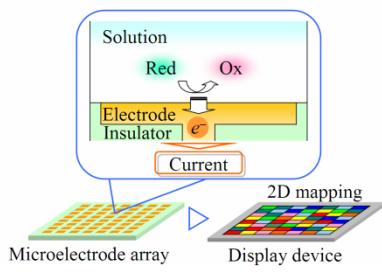
Microelectrode array   Display device

Fig. 1 Schematic of amperometric sensor device. Red and Ox denote reductant and oxidant, respectively. The goal of this study is to realize 2D imaging of analyte distributions by amperometry.
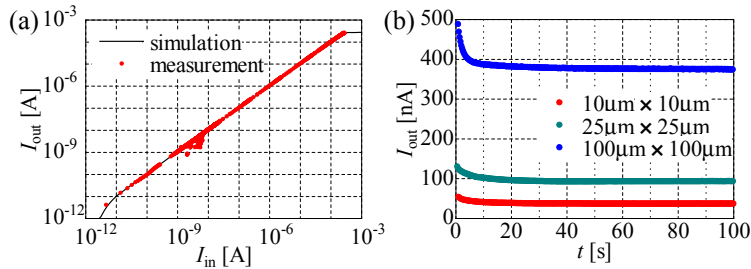
electrode1   swA1
    swB1
Current buffer circuit
electrode2   swA2
    swB2
Current buffer circuit   OA V_{out}

Fig. 2 Our amperometric electrochemical sensor circuit. Each electrode is connected to two switches. An electrode under measurement is connected to the readout circuit via "switch A", and otherwise the potential is fixed to maintain steady-state current via "switch B" during stand-by. Current buffer circuit suppress electrode voltage variation by switching.

(a)
V_{dd}
electrode
I_{in} V_{el} I_{out}
V_{ss}

(b) 99 μm
49 μm

Fig. 3 Current buffer circuit. (a) Schematic diagram. (b) micrograph. Chips were fabricated with a 1.2 μm, 2-poly, 2-metal standard CMOS process. This circuit employs the source follower to fix electrode potential at V_{el} as well as the current mirror to copy current ($I_{out}=I_{in}$).

(a) 10^{-3}
I_{out} [A]
simulation
measurement
10^{-6}
10^{-9}
10^{-12}
10^{-12} 10^{-9} 10^{-6} 10^{-3}
I_{in} [A]

(b) 500
I_{out} [nA]
400
300
200
100
0
10μm× 10μm
25μm× 25μm
100μm× 100μm
0 20 40 60 80 100
t [s]

Fig. 4 (a) Input-output characteristics of current buffer circuit. Input current range is between 10 pA and 100 μA, and measured input current agrees well with simulation in the range between 1 nA and 100 μA. (b) The time course of the electrochemical current of 100 mM Na_2SO_4 measured using current buffer circuit. On-chip gold microelectrodes (10μm× 10μm, 25μm× 25μm, and 100μm× 100μm), Ag/AgCl, and a Pt wire were used as working, reference, and counter electrodes, respectively. The output current increases with increasing electrode size.

(a)
WE (Anode)
Ox$^+$ Red$^-$
Anode

(b)
WE (Anode)
AE (Cathode)
Ox$^+$ Red$^-$ Red$^-$ Ox$^+$
Cathode Anode Cathode

Fig. 5 (a) Conventional microelectrode array. Diffusion layers of the closely spaced microelectrodes overlap. (b) Proposed microelectrode array. Working electrode (WE) is surrounded by insulated regions and a grid auxiliary electrode (AE), and redox cycling occurs between the electrodes.

(a)
Solution   Unit cell
z
y x
Electrode
Insulator

(b)
L_{unit} Unit cell
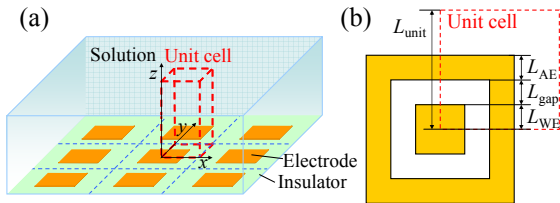L_{AE}
L_{gap}
L_{WE}

Fig. 6 (a) Computer simulation model. (b) proposed electrode geometry. The time-dependent diffusion problems solved by COMSOL Multiphysics (ver. 3.5, Comsol, Inc., Burlington, MA)

(a) 500
z [μm]
400
300
200
100
0
0 85
x [μm]

(b) 500
z [μm]
400
300
200
100
0
0 85
x [μm]
1
0

Fig. 7 Color maps of simulated concentration profiles along a side of the unit cell. The color bar indicates concentration in mM. (a) Conventional microelectrode array. The diffusion layers of the closely spaced microelectrodes overlap and planar diffusion layer is formed. (b) Proposed microelectrode array. Grid auxiliary electrode confine diffusion layer, and hemispherical diffusion layers are formed on individual microelectrode.

10^{-7}
I [A]
single eletrode
electrode array(conventional)
electrode array(this work)
10^{-8}
10^{-9}
L_{WE}:12.5μm L_{AE}:25μm
L_{gap}:5μm L_{unit}:85μm
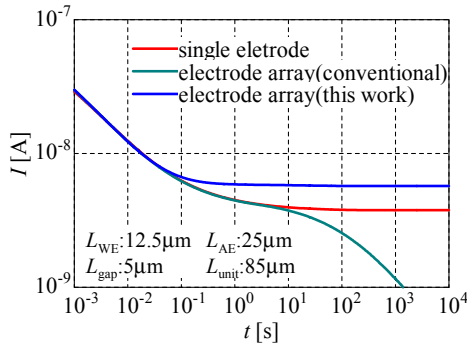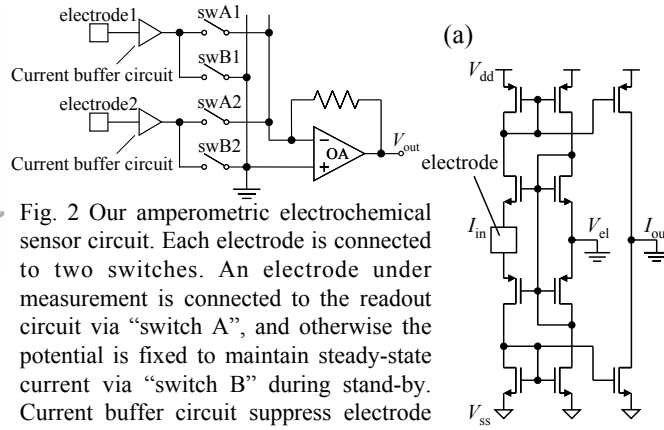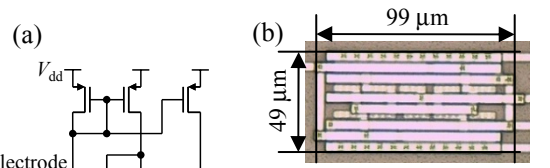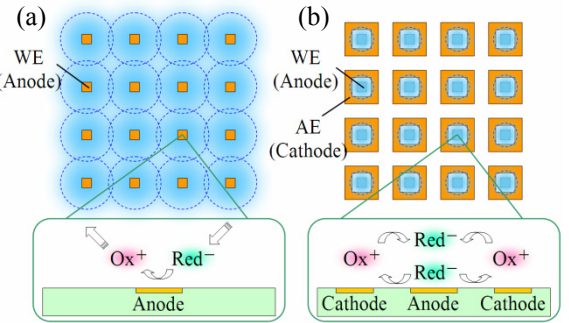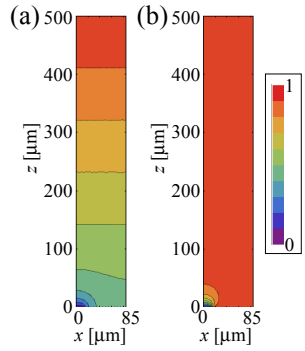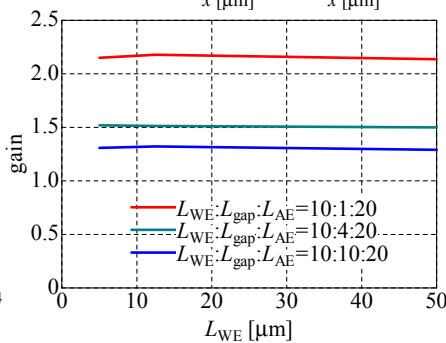10^{-3} 10^{-2} 10^{-1} 10^{0} 10^{1} 10^{2} 10^{3} 10^{4}
t [s]

Fig. 8 Simulation results of amperometry. Our MEA shows a steady-state current. Furthermore, the steady-state current is amplified compared to single microelectrode, and the time to reach the steady-state is reduced to about 1/10 of that of single microelectrode.

2.5
gain
2.0
1.5
1.0
0.5
0
0 10 20 30 40 50
L_{WE} [μm]
L_{WE}:L_{gap}:L_{AE}=10:1:20
L_{WE}:L_{gap}:L_{AE}=10:4:20
L_{WE}:L_{gap}:L_{AE}=10:10:20

Fig. 9 The ratio of steady-state current at proposed microelectrode structure to single microelectrode (gain) as a function of L_{AE}/L_{WE}. Gain depends on the ratio of three characteristic lengths of geometry; L_{WE}:L_{gap}:L_{AE}, rather than the absolute lengths.

2.5
gain
2.0
1.5
1.0
0.5
0
0 1.0 2.0 3.0 4.0
L_{AE}/L_{WE}
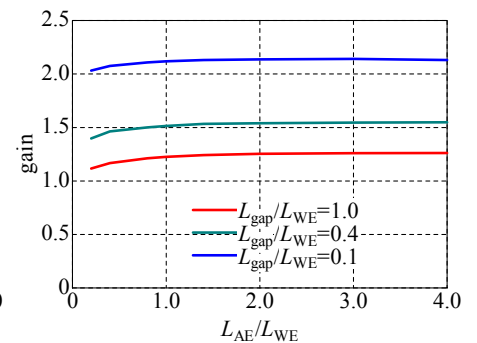L_{gap}/L_{WE}=1.0
L_{gap}/L_{WE}=0.4
L_{gap}/L_{WE}=0.1

Fig. 10 Gain as a function of L_{AE}/L_{WE}. The gain saturates at L_{WE}/L_{AE} = 1.0. As L_{gap}/L_{WE} decreases, larger amplification is observed.